Infectious Disease Modelling 9 (2024) 397–410

Contents lists available at ScienceDirect

Infectious Disease Modelling

journal homepage: www.keaipublishing.com/idm

A novel approach to model the role of mobility suppression and vaccinations in containing epidemics in a network of cities

Leen Alrawas [a], Abdessamad Tridane [b, c, *], Ghassane Benrhmach [d]

[a] Department of Physics, New York University Abu Dhabi, Abu Dhabi, Abu Dhabi, United Arab Emirates
[b] Department of Mathematical Sciences, United Arab Emirates University, Al Ain, Abu Dhabi, United Arab Emirates
[c] Emirates Center for Mobility Research, United Arab Emirates University, Al Ain, Abu Dhabi, United Arab Emirates
[d] Department of Statistics and Business Analytics, United Arab Emirates University, Al Ain, Abu Dhabi, United Arab Emirates

ARTICLE INFO

Article history:
Received 5 October 2023
Received in revised form 12 December 2023
Accepted 14 January 2024
Available online 7 February 2024
Handling Editor: Dr Yijun Lou

Keywords:
Agent-based modeling
Network
Epidemics

ABSTRACT

This paper presents a comprehensive agent-based model for the spread of an infection in a network of cities. Directional mobility is defined between each two cities and can take different values. The work examines the role that such mobility levels play in containing the infection with various vaccination coverage and age distributions. The results indicate that mobility reduction is sufficient to control the disease under all circumstances and full lockdowns are not a necessity. It has to be reduced to different ratios depending on the vaccination level and age distribution. A key finding is that increasing vaccination coverage above a certain level does not affect the mobility suppression level required to control the infection anymore for the cases of young population and heterogeneous age distributions. By investigating several migration and commuting patterns, it is found that shutting mobility in a few local places is favored against reducing mobility over the entire country network. In addition, commuting -and not migration-influences the spread level of the infection. The work offers an exclusive combined network-based and agent-based model that makes use of randomly generated mobility matrices.

1. Introduction

The primary response made towards disease outbreaks is to imply full lockdowns to restrict the transmission of the disease (Bhadoria, Gupta, & Agarwal, 2021). Although preventing contact between people can suppress the disease, it has serious psychological and economical drawbacks that may last for decades. As a recent example, the coronavirus pandemic (Covid-19) resulted in serious socio-economic implications (Nicola et al., 2020). Therefore, more flexible and effective strategies to control infections and prevent disease outbreaks are needed. Furthermore, the spread of infections often relates to a person's age and health status (El-Gendy et al., 2020; Fox, Cooney, Hall, & Foy, 1982; Hutchins et al., 2020; Kada, Kouidere, Balatif, Rachik, & Labriji, 2020). Hence models that account for differences in population demographics are necessary to

* Corresponding author. Department of Mathematical Sciences, United Arab Emirates University, Al Ain, Abu Dhabi, United Arab Emirates.
E-mail addresses: laa9597@nyu.edu (L. Alrawas), a-tridane@uaeu.ac.ae (A. Tridane), g.benrhmach@uaeu.ac.ae (G. Benrhmach).
Peer review under responsibility of KeAi Communications Co., Ltd.

https://doi.org/10.1016/j.idm.2024.01.005

provide an adequate representation of disease transmission. In addition to mobility control, nonpharmaceutical interventions include vaccinating the population against the infection. Vaccinations can also vary in their efficiency and coverage between populations and a combined effect of mobility suppression and vaccines has to be examined.

Numerous studies have shown the correlation between human mobility and the evolution of epidemics (Guo, Deng, & Gu, 2022; Jewell et al., 2021; Kissler et al., 2020; Nouvellet et al., 2021). A previous study shows that directional mobility between two cities affects the global and local epidemic sizes in different ways (Espinoza, Castillo-Chavez, & Perrings, 2020). Another recent study (Pardo-Araujo, García-García, Alonso, & Bartumeus, 2023) uses random matrix theory to examine two types of human mobility patterns and derive analytical thresholds. The work (Jewell et al., 2021) concludes that mobility is not a reliable indicator of infection rates. In addition, population age distributions and vaccination levels tend to play a crucial role in deciding the best control strategies (Guo et al., 2022; Patel et al., 2021; Zhang et al., 2022). Vaccination coverage was particularly found impactful in reducing infection risks. In (Patel et al., 2021), the authors showed that high coverage with low vaccination efficacy is more powerful than low coverage with high efficacy. The study also clearly shows the significance of maintaining control strategies while vaccinating the population. Mobility between regions is frequently generated using mobility networks with weighted directed graphs where nodes represent geographical locations and edges represent mobility flows between locations (Ganciu, Balestrieri, Imbroglini, & Toppetti, 2018; Martin, Wiedemann, Reck, & Raubal, 2023; Mauro, Luca, Longa, Lepri, & Pappalardo, 2022). The topology of such networks has a significant impact on the epidemic's spread (Moreno, Pastor-Satorras, & Vespignani, 2002). Data-driven network-based models were frequently combined with machine learning and deep learning techniques to uncover important patterns and conclusions in specific geographical districts (Anno, Hirakawa, Sugita, & Yasumoto, 2022; Ojugo & Nwankwo, 2021; Pinheiro, Galati, Summerville, & Lambrecht, 2021; Roy, Biswas, & Ghosh, 2021). Another common modeling method that has been used in epidemiological studies is agent-based modeling (Chen et al., 2022; Patel et al., 2021; Vedam & Ghose, 2022). It represents a detailed description of contagions spread by tracing agents (individuals) and can be highly adjustable to include different nonpharmaticual interventions and assess their relative effects. A former study (Chen et al., 2022) proposed a multi-layer network that considers both social contact (using an agent-based approach) and urban commuting (using a time-varying network). Employing available vaccine cases, the study examined several control strategies individually and reported their effectiveness. As an example, the results show that preventing disease outbreak requires more than a 50% reduction in public transport systems.

The present model proposes a network of cities where weighted matrices connect local populations. The model was not designed to match a certain location but rather offers a platform to draw general conclusions and can be easily adjusted to match specific regions. Two matrices are considered analogous to the work of Garcia et al. (Pardo-Araujo et al., 2023) to reflect two kinds of human movement: commuting where people move to another city temporarily and return to their home city afterward, and migration where people move permanently from one place to another. The movement patterns comprise a Movement-Interaction-Return (MIR) model (Ojugo & Nwankwo, 2021). The model also considers different vaccination cases and age distributions and investigates their combined contribution to the infection outspread. The different cities are presented as different simulations (separate code runs) that can run and interact simultaneously to allow movement. The novelty of this approach allows high flexibility in choosing the size of the network and properties of the sub-populations. The network weighted matrices are generated randomly to model variability in human mobility. To enhance the complexity of the model, the random network is combined with a stochastic disease transmission model using agent-based modeling.

The model provides a valid predictive and assessing tool for policymakers to control epidemics under various circumstances. In the present work, we study the mobility levels required to control the infection in several vaccination and age cases. Moreover, we investigate how different commuting and migration patterns affect the infection level.

The paper is sectioned as follows: first, we define the model methodologies and parameters by providing a description of the model. Then, we describe the methods applied in the sensitivity analysis, the optimization, and the analysis of different commuting and migration scenarios respectively. In the Results section, we present the outcomes. Finally, the conclusion provides a summary of the results.

2. Materials and methods

2.1. Model description

This study simulates a country with a number of patches, each representing a city. The cities are constructed separately, with one city being one simulation. This method of defining the different regions allows dealing with thousands of agents with ease and prevents errors that can happen in calculations due to a low number of agents making the model more robust. The simulations were coded and run in GAMA Platform 1.9 - Windows 10 64-bit operating systems - Processor: Intel(R) Core(TM) i7-8550U CPU @ 1.80 GHz.These simulations interact with each other to allow mobility between patches. The sizes of the cities, the population (size and age), and the disease parameters can all be defined differently for each city. The model also allows the user to specify the number of cities. We assume patches with a square shape of side length 1000 m. The population is assumed to be the same: 1000 susceptible in each patch and a random choice of 3,4, or 5 infected agents in each patch. The age distribution can be different in each patch. By default, we assume a normal age distribution for all patches with

Table 1
The population age groups.

Age Group	Age Range
1	[0, 5]
2	(5, 15]
3	(15, 55]
4	(55, 70]
5	+70

a mean age of 40 and a standard deviation of 15. To avoid negative age, an age of 0 is assigned for each negative value chosen by the random generator. Furthermore, the population is divided into five age groups (Table 1).

Susceptible agents can get exposed to the disease if they get close to an infected agent, or they can get vaccinated. Exposed agents will eventually be infected then they recover from the disease. Vaccinated agents can either become immune or exposed to the infection due to imperfect vaccinations when they get close to infected agents. The flowchart of the model is demonstrated in Fig. 1. To match the model with COVID-19 characteristics, it was found neighbors should be defined at a distance <20 m from the agent. The probabilities of changing the agent's state are shown in Table 2. In Tables 2 and IN is the number of infected neighbors, and CAI is the difference between the age group index of the agent and that of a neighbor infected agent of the closest age. Getting exposed depends on age since agents of the same age group tended to infect each other (Monod et al., 2021). Taking COVID-19 as an example, it was found that exposure tends to be age-dependent (Jing et al., 2020). The values reported in the study are considered as a guide for the age risk. Considering the population aged >60 years as a reference (probability is 1), people aged between 20 and 59 years have a 0.64 probability of being exposed, and younger populations aged <20 years have a 0.23 probability of being exposed.The efficacy of vaccination is represented by the parameter λ in the flowchart 1. It takes a random value between 0.65 and 0.95 as the vaccination effect varies between agents based on several factors including age and health status.

2.2. Mobility of agents

Mobility is the main cause of the spread of infection between agents. A susceptible agent can get exposed to the disease if it gets close to an infected agent. All agents are allowed to move locally in their current patches. Local mobility can be controlled by changing the value of the parameter *local-mobility* that represents the ratio of moving agents in a patch. This value is assumed to be uniform over all patches and the default value is 1.

There are two other types of mobility that occur between different patches: commuting and migration. Infected agents are not allowed to leave their patches while they are still infected. However, mobility between patches can still spread the disease because the exposed agents can travel and transmit the disease later when they get infected. This means the exposed agents also include agents who are asymptomatic. All patches are assumed to be connected to one another within a network with a

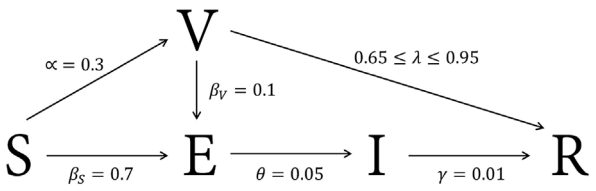

Fig. 1. The model flowchart.

Table 2
The probabilities of changing the agent's disease state.

	Probability
Susceptible to Exposed	$(1-(1-\beta_s)^{\text{IN}}) \times (1-\frac{\text{CAI}}{5}) \times \text{age} - \text{risk}$
Vaccinated to Exposed	$(1-(1-\beta_v)^{\text{IN}}) \times (1-\frac{\text{CAI}}{5}) \times \text{age} - \text{risk}$
Exposed to Infected	θ
Infected to Immune	γ
Susceptible to Vaccinated	α
Vaccinated to Immune	λ

weighted graph. We quantify two matrices for the network to represent commuting (P_{ij} matrix) and migration (M_{ij} matrix) that have the following format, assuming we have N patches:

$$P = \begin{bmatrix} P_{11} & P_{12} & .. & P_{1N} \\ P_{21} & P_{22} & .. & P_{2N} \\ : & : & : & : \\ P_{N1} & P_{N2} & .. & P_{NN} \end{bmatrix} \tag{1}$$

$$M = \begin{bmatrix} M_{11} & M_{12} & .. & M_{1N} \\ M_{21} & M_{22} & .. & M_{2N} \\ : & : & : & : \\ M_{N1} & M_{N2} & .. & M_{NN} \end{bmatrix} \tag{2}$$

In the commuting matrix P, each entry P_{ij} represents the proportion of people in patch i who are allowed to move to patch j per unit time (taken to be one day). The entries P_{ij}'s are a reflection of the probability per day that an agent in patch i moves to patch j relatively to other patches and the values are independent (they do not represent a real probability as explained in (3) and hence they don't need to sum to 1 for each patch). The diagonal entries denote the proportion of agents who stay in their patch. A sample illustrative network graph with four patches is demonstrated in Fig. 2. Commuting means that agents return to their original patch after some time. We assume a probability of 0.01 (per day) for returning home when an agent travels to another patch. Furthermore, to reflect a realistic situation, we assume that the probability of an agent moving to one random patch per day should not exceed 0.25 at all times. That is, no more than 1/4 of the patch population is allowed to move out at once. Therefore, we add a condition on matrix entries to be less than or equal to 0.25 (excluding the diagonal entries).

$$\text{probability of leaving a patch per day} \leq 0.25 \tag{3}$$

This value can be changed depending on the case to be studied. This condition is always satisfied regardless of the row sums of P_{ij} values in the commuting matrix.

For agents who have already moved to another patch using the matrix P there is a M_{ij} probability that this travel was migration and that the agent does not return home after. If true, the state of the agent is changed to *migrated*. Once an agent is marked as migrated, their original patch changes to the one they are currently in and they do not have to return to their previous patch as described in the section above. The probability that an agent in patch i migrates to patch j (per day) is hence $P_{ij} \times M_{ij}$, given that no more than 1/4 of the patch population leaves the patch (3).

Moving agents between patches is not done directly since the patches are defined as separate simulations. Instead, to move an agent we remove the agent from its current simulation, then we create an identical agent in the new simulation

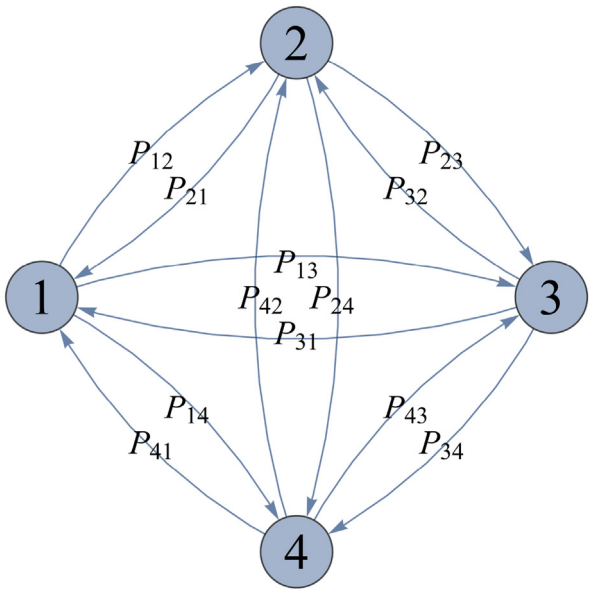

Fig. 2. A network of four cities with directed edges representing commuting mobility between cities with values from matrix (1).

while preserving all of its properties. In spatial models where the regions are defined in one simulation, the mobility of agents also requires that the agent is existent close to an exit path. In the present model, this requirement is eliminated making the model more well-defined.

The entries of the commuting and mobility matrices are generated randomly in an external software when the model is initialized. The matrices are then uploaded to the simulation and assumed to remain constant during the simulation run. Different conditions are applied to the random generation to describe certain scenarios where needed.

Mobility between patches is restricted based on age: agents from age 0 to 5 and with ages higher than 70 can't leave their patches, people aged between 15 and 55 (inclusive of 55) have the highest probability of traveling between patches (80 percent), and the rest of the population has a probability of 40 percent of traveling.

2.3. Infection metrics

We use the five metrics to quantify the severity of the infection spread: the basic reproduction number R_0, the prevalence, the time of the peak, the size of the peak, and the effective time-dependent reproduction number (Thompson et al., 2019). the basic reproduction number is a well-known epidemiological parameter that denotes the expected number of new infections produced by a single infectious agent. In the model, R_0 is defined per patch as follows (Al-Shaery, Hejase, Tridane, Farooqi, & Jassmi, 2021):

$$R_0 = \frac{\text{number of infected agents}}{\text{number of active infected agents}} \tag{4}$$

where *active* denotes the cumulative number of infected agents who have infected healthy agents, and the number of infected agents is the cumulative number of newly infected agents.

The probability of an infected agent being active is $1-(1-\beta_s)^{\mathrm{SN}} \times (1-\frac{\mathrm{CAS}}{5})$ where SN is the number of susceptible neighbors, and CAS is the difference between the age group index of the agent and that of a susceptible neighbor agent of the closest age (close age susceptible). The global R_0 is defined as the average of the local R_0 values.

The effective reproduction number R_{eff} changes with time and has the same definition as R_0 except that in this case, we do not take the maximum as in the case of R_0. In other words, R_0 is simply the maximum value of R_{eff} reached throughout the simulation.

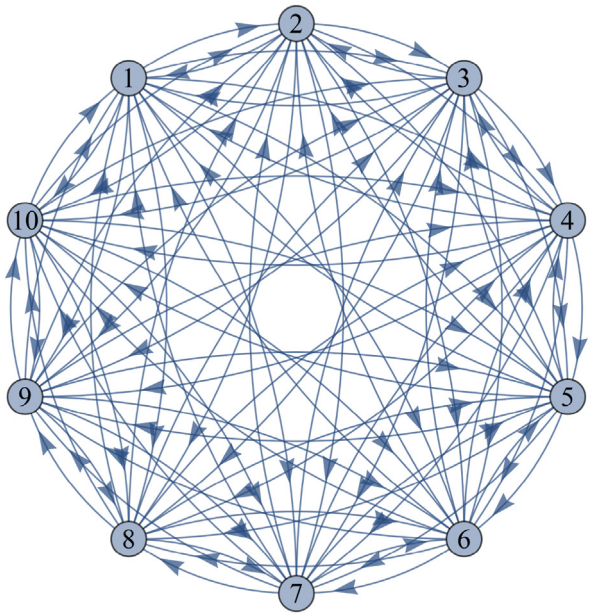

Fig. 3. A complete network of ten cities with directed edges representing mobility between cities (commuting or migration).

The prevalence represents the level of infection and is defined by:

$$\text{Prevalence} = \frac{\text{number of all infected agents}}{\text{number of all agents}} \tag{5}$$

where the number of all infected agents denotes the total global infected agents since the beginning of the simulation.

Table 3
The range of parameter values investigated in the sensitivity analysis.

Parameter	Value in Model	Min	Max	Increment
A	0.3	0.1	0.5	0.05
β_s	0.7	0.3	0.8	0.05
β_v	0.1	0.02	0.2	0.02
Θ	0.05	0.01	0.1	0.01
Γ	0.01	0.002	0.02	0.002
λ (the vaccination efficacy)	random	0.5	0.9	0.05
Age-mean	40	15	70	5
Age-SD	15	2	30	2

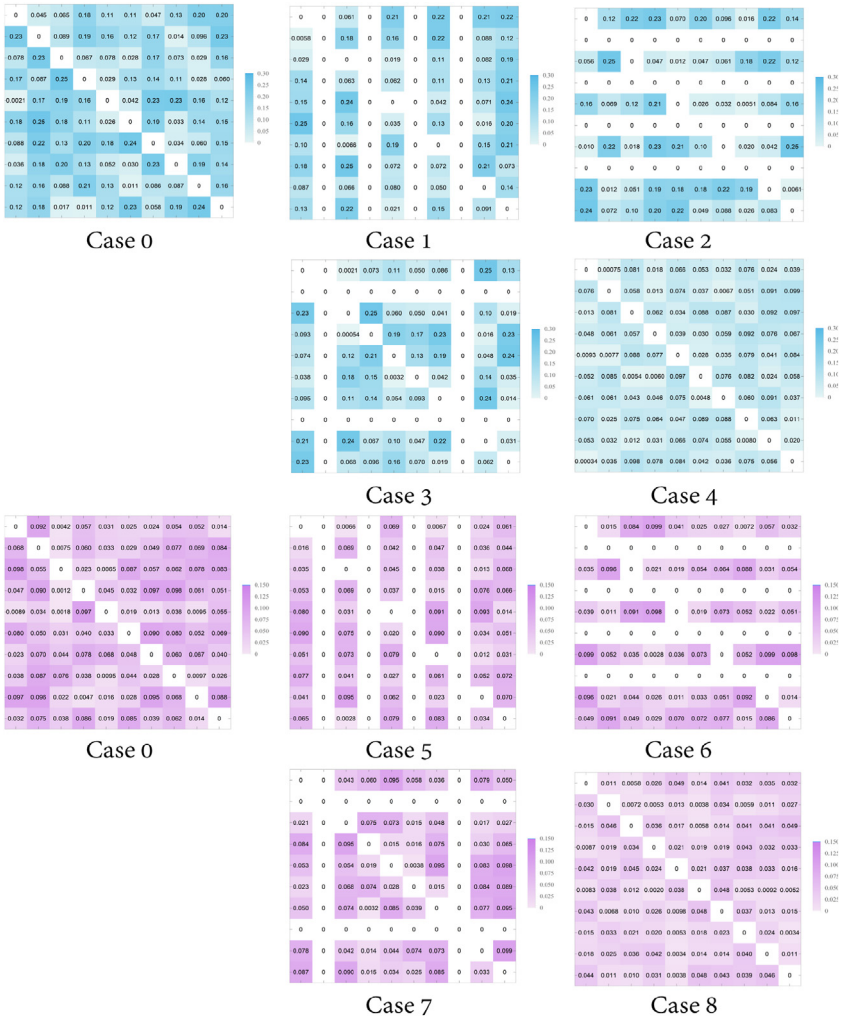

Fig. 4. The network matrices of different commuting (blue) and migration (purple) cases - case 0 is the base scenario.

2.4. Sensitivity analysis

Using 10 patches each with 1000 susceptible agents and three to five infected agents (see Fig. 3), we perform the local (point-based) sensitivity analysis. The values of the parameters are varied one by one on their reasonable range and the output metrics are measured in each case. For visualization and comparison, we plot the parameter values scaled to an interval of [0,1] on the x-axis and the output of interest on the y-axis (refer to the Appendix for full results). The analysis is done twice: one without vaccination, and one with vaccination taking the vaccination coverage to be 50% in each patch. Table 3 shows the ranges of parameter values that were considered.

2.5. Optimization method

We aim to find the optimal mobility structure between cities that allows disease control. For that reason, we define another metric to restrict mobility: *the critical infection ratio* (CIR). In a patch, we measure the level of the infection; the ratio of infected people, if this value is less than CIR then agents are allowed to leave their patch, otherwise, they cannot leave their patch. Using a constant CIR value, we can measure the number of trips made between patches throughout the simulation and construct a mobility matrix similar to 1. Initially, we use a CIR value of 1 (maximum mobility) and we measure the initial mobility matrix and the possible outputs. Then, we aim to find the value of CIR that permits the control of the infection globally with the maximum possible mobility. This means we want to find the maximum level of mobility that results in $R_{0,global} < 1$. Since the control variable is the CIR, it is feasible to construct a table of possible values of CIR (from 0 to 1) with their outcomes and find the maximum value of CIR that still gives $R_{0,global} < 1$.

To represent a realistic situation, mobility reduction is aimed to control a country where the disease initially starts in several cities. We assume 10 patches each with 1000 agents and we initiate the infection in three of them. Since the age of the population plays a crucial role in the spread of the pandemic, we consider several scenarios for the optimization based on different age distributions.

1. The mean age is uniform across cities and is taken to be 30.
2. Similar to the first case with a mean age of 50.
3. The initially infected patches have a mean age of 50, and the rest have a mean age of 30.
4. The initially infected patches have a mean age of 30, and the rest have a mean age of 50.
5. Random mean age for all cities.

2.6. Commuting and migration different scenarios

We investigate the response of the system to several commuting and migration networks. In all scenarios, we compare the spread of the infection to a base case using time series of the infected population and the effective reproduction number R_{eff}. The cases are implemented by changing the structures of the mobility matrices $P(1)$ and $M(2)$. The entries of the matrices are generated randomly between 0 and a maximum value that is chosen depending on the desired case. The disease is initialized in one city at the beginning of the simulation. We simulate 10,000 agents distributed in 10 cities.The following scenarios are considered (Fig. 4).

1. Shutting down inward commuting flows in four nodes.
2. Shutting down outward commuting flows in four nodes.
3. Shutting down both inward and outward commuting flows in two nodes.
4. Reducing commuting flows uniformly over the entire network.
5. Shutting down inward migration flows in four nodes.
6. Shutting down outward migration flows in four nodes.
7. Shutting down both inward and outward migration flows in two nodes.
8. Reducing migration flows uniformly over the entire network.

3. Results

3.1. Sensitivity analysis

The bar charts in Figs. 5–8 summarize the sensitivity analysis results for each of the chosen outputs where R^2 is the coefficient of determination. The coefficient of determination is determined by plotting the output of choice versus the parameter over its range scaled from 0 to 1. Full results are available in the Appendix.The age distribution parameters (mean

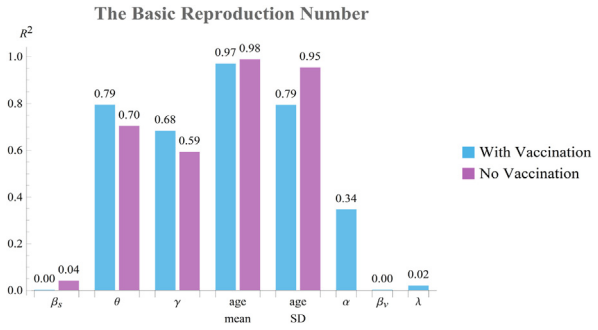

Fig. 5. The coefficient of determination R^2 for the relation between different parameter values and the basic reproduction number.

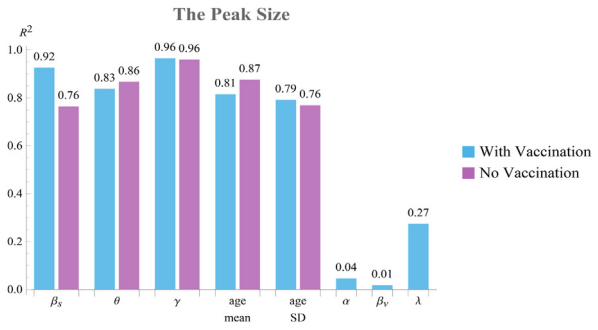

Fig. 6. The coefficient of determination R^2 for the relation between different parameter values and the peak of the disease.

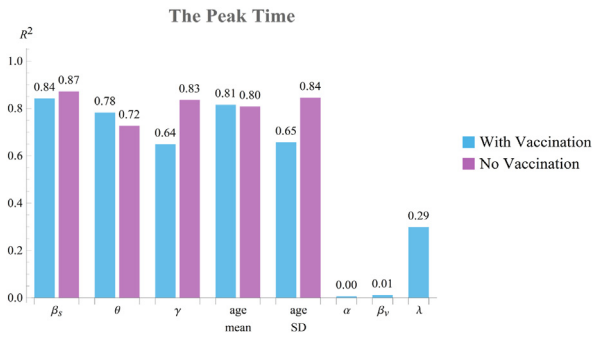

Fig. 7. The coefficient of determination R^2 for the relation between different parameter values and the infection peak time.

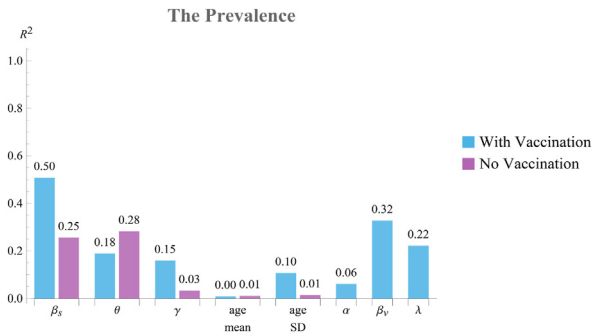

Fig. 8. The coefficient of determination R^2 for the relation between different parameter values and the global prevalence.

and standard deviation) tend to have the most effect on R_0. The peak size and time are more sensitive to changes in parameter values. The peak size is mostly sensitive to the infection rate β_s and the recovery rate γ. Finally, the prevalence is the most robust and is mostly affected by the infection rates for susceptible β_s and vaccinated agents β_v in the case of having a vaccinated population. Generally, the presence of the vaccination does not play a role in changing the level of sensitivity to different parameter values.

3.2. Optimization outcomes

We measure the number of trips made between every two patches when mobility is fully relaxed and when mobility is restricted to achieve a value of R_0 less than one using the suitable CIR value (see Methods). The number of trips made between patches is not necessarily a good indicator of the mobility level as the pandemic may last longer in some cases allowing more trips to be made even if the mobility level throughout the simulation is lower. To solve this, we represent the mobility level as the number of trips made per unit time (dividing the number of trips by the simulation duration). The simulation ends when the disease dies out, that is when the number of infected people decreases below 2. The mobility level is summarized in a matrix where each matrix entry x_{ij} represents the number of trips made from patch i to patch j per unit time. The figures demonstrate the results of sample runs and the values of R_0 before and after mobility suppression are recorded in the bar charts after taking the average over several runs.Various age and vaccination coverage cases are considered. The outcomes show that a reduced mobility level can help contain the disease and keep the pandemic under control by having $R_{0,global} < 1$. The level of mobility depends on how much the infection has expanded in the simulation and the level of vaccination. When a patch becomes highly infected, a much lower mobility level out of the patch is required. The results are recorded while keeping the input matrices $P(1)$ and $M(2)$ constant. The assigned value is 0.01 for both matrices. We present the matrices for the case of a uniform mean age of 30 (Fig. 9), other cases are available in the Appendix.

The results can be summarized as follows.

- **Case 1 (uniform mean age of 30)**: When 75% of the population is vaccinated, mobility has to be reduced to about 40% of the level of fully relaxed mobility. A similar pattern is observed for vaccination coverage of 50%, but the original mobility level is a little less in this case. For 25% and 0% vaccination levels, mobility has to be reduced to approximately 30% and 25% of the original value respectively.
- **Case 2 (uniform mean age of 50)**: For old populations, mobility has to be reduced more in all vaccination cases. Depending on the vaccination coverage, its level should decrease to 20%–30% of the fully relaxed mobility.
- **Case 3 (infected patches mean age is 30, the rest is 50)**: When the disease initially starts in younger populations, a similar pattern is observed as in Case 1 where all populations are young. Mobility levels are all slightly lower in this case.
- **Case 4 (infected patches mean age is 50, the rest is 30)**: Mobility is also less in this case compared to Case 3 for both situations: when fully relaxed and when suppressed. Again the ratio of suppressed mobility to relaxed mobility has similar trends to Case 1 and Case 3.
- **Case 5 (random mean age)**: When each city has a different random age distribution, different vaccination levels do not make a significant impact on the outcomes. The mobility has to be reduced to about 35% for a vaccination percentage of 75 and to about 30% for all other cases.

3.3. Commuting and migration scenarios outcomes

Eight scenarios for different commuting and migration levels are investigated (see Methods). The cases are demonstrated in Fig. 4. The outcomes are summarized based on the global infection, the effective reproduction number R_{eff}, and the local distribution of the disease. Figs. 10, 11 and 12 show the results where case 0 represents the base scenario.

- R_{eff}: Shutting down both inward and outward mobility in two nodes helps reduce R_{eff} below 2 (case 3) where in the base case, R_{eff} reaches about 2.3. Another way to reduce R_{eff} is to shut down inward commuting flows in selected nodes (case 1). Shutting down outward commuting flows concentrates the disease in a few nodes which increases R_{eff} (case 2). In this case, R_{eff} increases steadily over time. Reducing commuting overall reduces R_{eff} slightly (only by 0.1). Different migration patterns do not play a role in controlling the infection. The maximum reduction is when migration is uniformly reduced (case 8) and is about 0.2.
- **The global infection**: The maximum decline in the peak happens for case 3 where commuting is blocked in both directions in selected nodes, followed by case 2 where only outward commuting flows are restricted. The rest of the

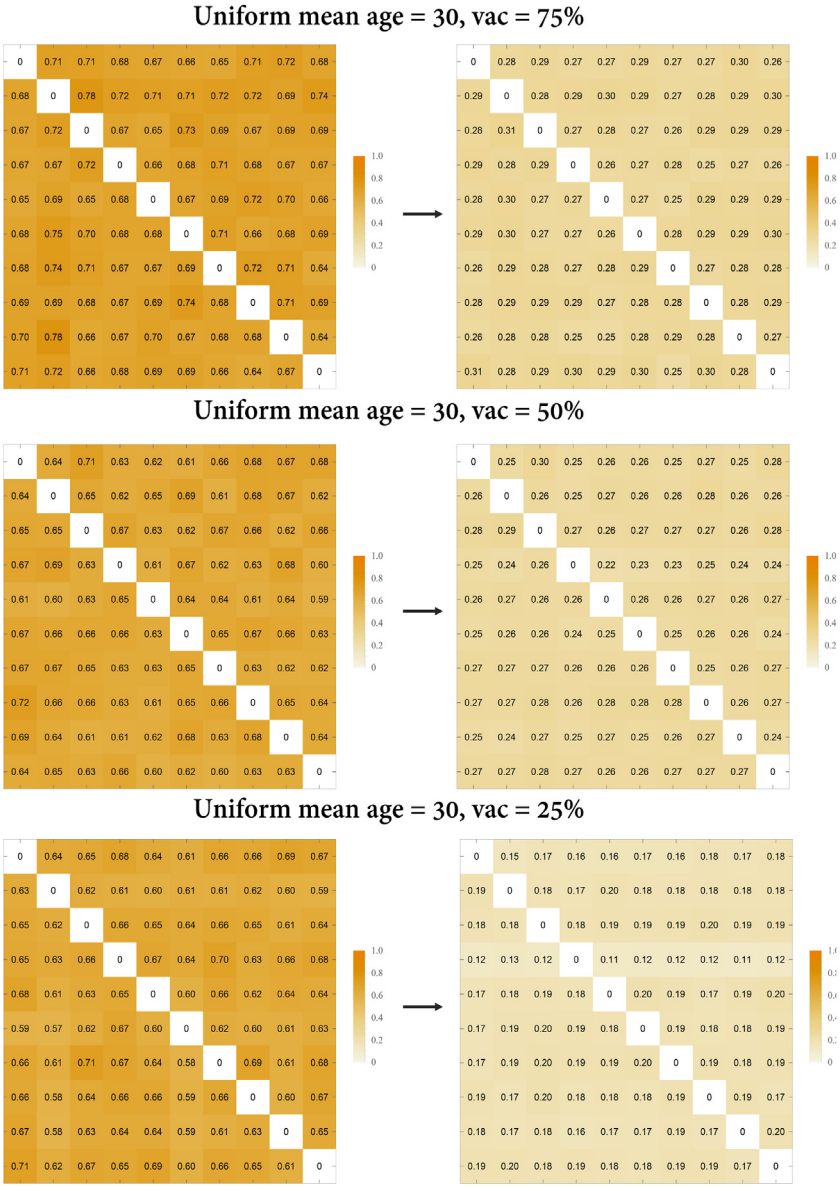

Fig. 9. Optimization results for the case of uniform mean age = 30.

commuting and migration cases do not change the global infection significantly; there is only a very small reduction in the peak. Overall, there is no effect on the time of the peak.

- **The local infection**: The infection is least distributed among cities in case 2 where outward commuting flows are blocked. Case 1 follows where inward commuting flows are blocked. Different migration scenarios result in slightly different disease distribution. The infection distribution is mostly varied between patches in the case where migration is uniformly reduced over the entire network (case 8).

4. Conclusion

We defined a new parameter: the *critical infection ratio* (CIR), which is used to conditionally suppress mobility based on the infection level in cities. This method showed that partial lockdowns are effective in controlling the epidemic under all circumstances and they should be concentrated in highly infected regions. A previous study (Roy et al., 2021) which

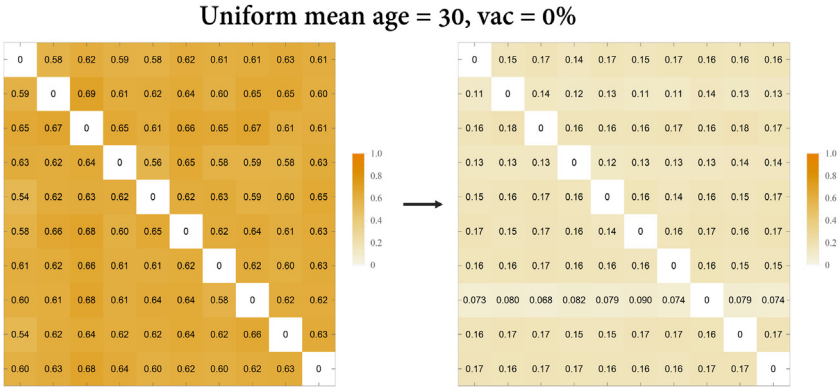

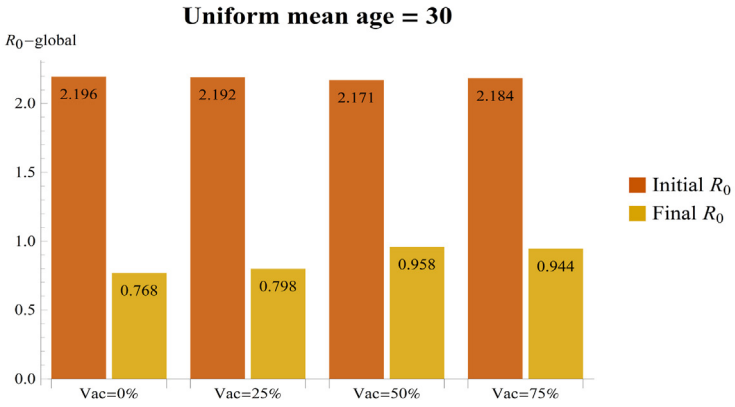

Fig. 9. (*continued*).

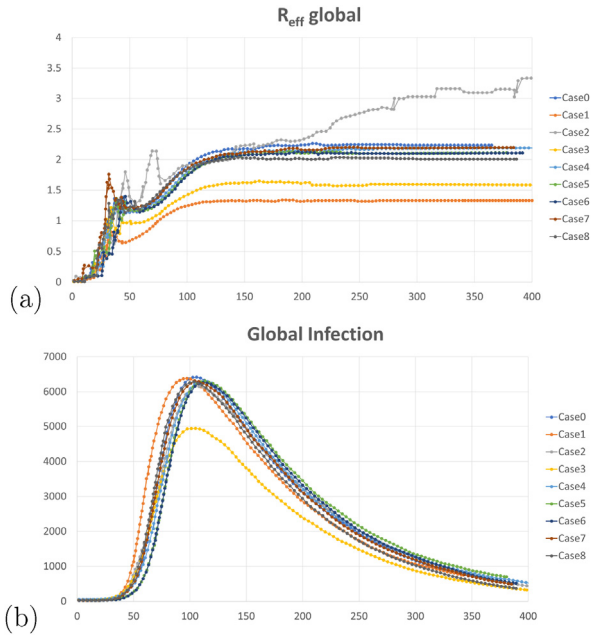

Fig. 10. The graphs of (a) R_{eff} and (b) the global infection over time for several migration and commuting scenarios (Fig. 4).

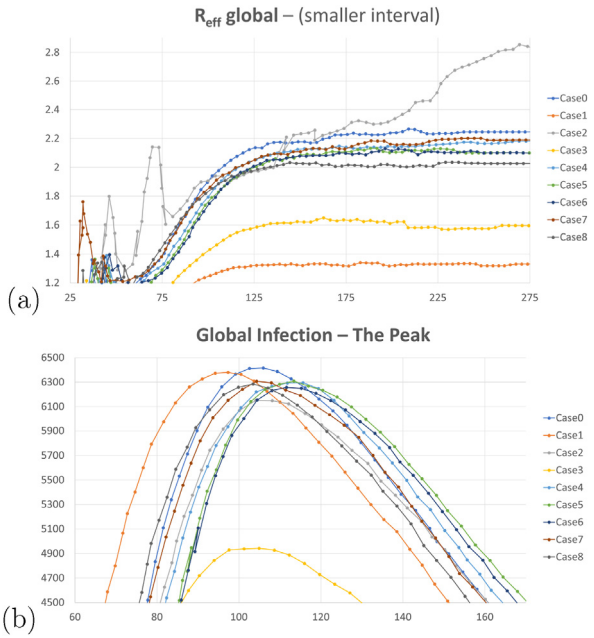

Fig. 11. The emphasized graphs around the peak of (a) R_{eff} and (b) the global infection over time for several migration and commuting scenarios (Fig. 4).

employed machine learning and a network-based approach to mitigate an infection in New York City counties has also found that mobility restriction strategies that are based on infection cases outperform the ones using random suppression patterns.

The extent of mobility reduction is related to both age and vaccination coverage and it ranges between 20% and 40% of the original relaxed level. High vaccination coverage after a certain level (about 50%) does not impact anymore how much mobility should be reduced in order to keep the disease contained in most cases, however, it still plays a role in reducing the number of infections and the peak size as expected. In the situation of old populations, mobility should be drastically decreased compared to other cases to control the disease spread.

The study also discussed the impact of a plethora of human movement patterns. It extends the work (Pardo-Araujo et al., 2023) which investigated the same using random matrix theory. In the present work, stochasticity was added to the system instead of a deterministic approach using an ABM. The present study shows similar general patterns even with more complex local and global mobility behaviors which emphasizes the results. Migration does not affect the infection level, it can only vary how the infection is distributed among cities. Reducing migration uniformly across the country makes the infection more distributed compared to other scenarios. Stopping commuting from selected cities in both directions was found to be more effective in reducing the infection than lowering commuting flows between all cities. In other words, local lockdowns comprise a functional strategy to control epidemics and reduce the number of infections in a network of cities.

The results of the study can be crucial for public health officials in making decisions related to epidemic control. The proposed model comprises a platform that can be calibrated to match different population demographics and country structures when data is available, in addition to its flexibility in considering various mobility and vaccination cases.

Despite the possibility of choosing any number of cities and any (possibly nonuniform) mobility level between them, the cities' geographical shape was omitted and a general shape was assumed and unified for all places. A future study may account for different geographical shapes. Moreover, the present study only investigated different mobility patterns *between* cities. Another approach may be including different mobility patterns *within* cities as well.

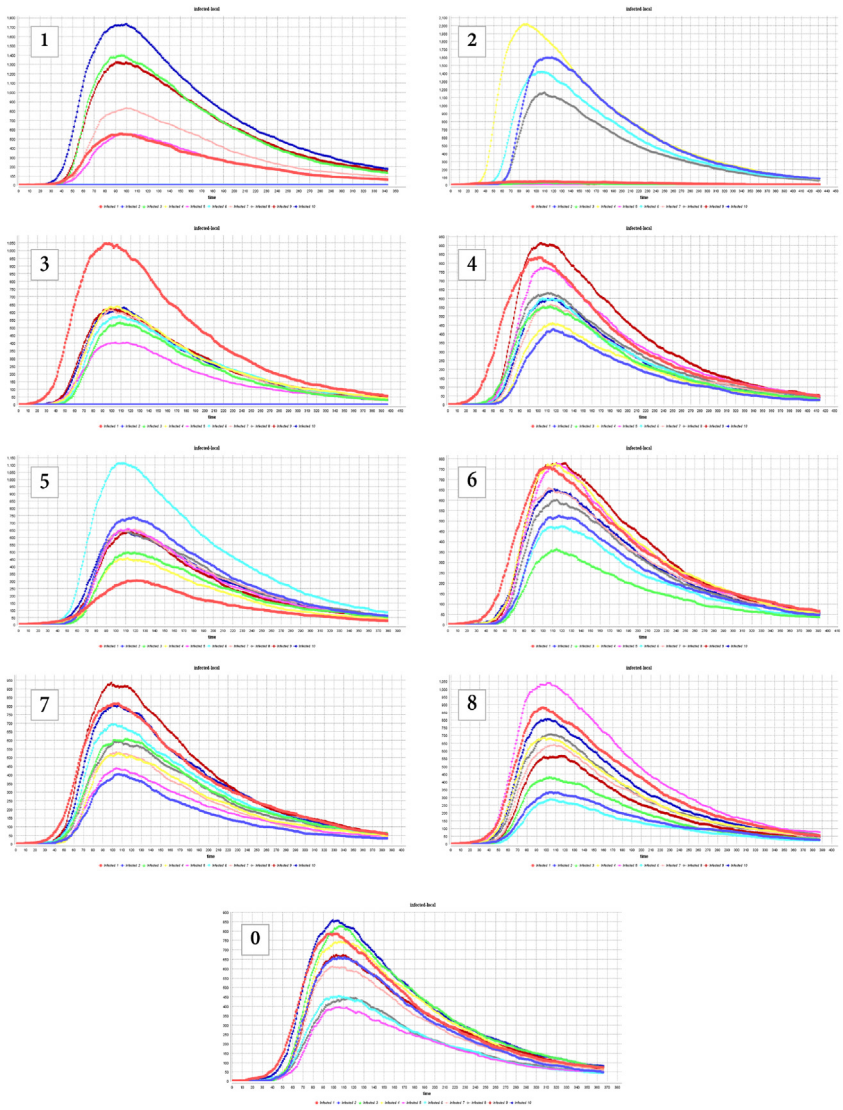

Fig. 12. The graph of the local infection over time for several migration and commuting scenarios (Fig. 4).

Funding

A. Tridane was supported by the UAEU UPAR, grant number 12S125.

CRediT authorship contribution statement

Leen Alrawas: Conceptualization, Formal analysis, Investigation, Software, Visualization, Writing – original draft, Writing – review & editing. **Abdessamad Tridane:** Conceptualization, Data curation, Formal analysis, Funding acquisition, Methodology, Project administration, Resources, Supervision, Validation, Writing – original draft, Writing – review & editing. **Ghassane Benrhmach:** Formal analysis, Investigation, Methodology, Software, Visualization, Writing – review & editing.

Declaration of competing interest

The authors declare that they have no known competing financial interests or personal relationships that could have appeared to influence the work reported in this paper.

Acknowledgement

The authors would like to thank the anonymous reviewers for their valuable comments.

Appendix A. Supplementary data

Supplementary data to this article can be found online at https://doi.org/10.1016/j.idm.2024.01.005.

References

Al-Shaery, A. M., Hejase, B., Tridane, A., Farooqi, N. S., & Jassmi, H. A. (2021). Agent-based modeling of the hajj rituals with the possible spread of covid-19. *Sustainability, 13*(12), 6923.
Anno, S., Hirakawa, T., Sugita, S., & Yasumoto, S. (2022). A graph convolutional network for predicting covid-19 dynamics in 190 regions/countries. *Frontiers in Public Health, 10*.
Bhadoria, P., Gupta, G., & Agarwal, A. (2021). Viral pandemics in the past two decades: An overview. *Journal of Family Medicine and Primary Care, 10*(8), 2745.
Chen, P., Guo, X., Jiao, Z., Liang, S., Li, L., Yan, J., et al. (2022). A multilayer network model for studying the impact of non-pharmaceutical interventions implemented in response to covid-19. *Frontiers in Physics*, 687.
El-Gendy, A. O., Saeed, H., Ali, A. M., Zawbaa, H. M., Gomaa, D., Harb, H. S., et al. (2020). Bacillus calmette–guérin vaccine, antimalarial, age and gender relation to covid-19 spread and mortality. *Vaccine, 38*(35), 5564–5568.
Espinoza, B., Castillo-Chavez, C., & Perrings, C. (2020). Mobility restrictions for the control of epidemics: When do they work? *PLoS One, 15*(7), Article e0235731.
Fox, J. P., Cooney, M. K., Hall, C. E., & Foy, H. M. (1982). Influenzavirus infections in seattle families, 1975–1979: Ii. pattern of infection in invaded households and relation of age and prior antibody to occurrence of infection and related illness. *American Journal of Epidemiology, 116*(2), 228–242.
Ganciu, A., Balestrieri, M., Imbroglini, C., & Toppetti, F. (2018). Dynamics of metropolitan landscapes and daily mobility flows in the Italian context. an analysis based on the theory of graphs. *Sustainability, 10*(3), 596.
Guo, J., Deng, C., & Gu, F. (2022). Vaccinations, mobility and covid-19 transmission. *International Journal of Environmental Research and Public Health, 19*(1), 97.
Hutchins, H. J., Wolff, B., Leeb, R., Ko, J. Y., Odom, E., Willey, J., et al. (2020). Covid-19 mitigation behaviors by age group—United States, april–june 2020. *Morbidity and Mortality Weekly Report, 69*(43), 1584.
Jewell, S., Futoma, J., Hannah, L., Miller, A. C., Foti, N. J., & Fox, E. B. (2021). It's complicated: Characterizing the time-varying relationship between cell phone mobility and covid-19 spread in the us. *NPJ digital medicine, 4*(1), 152.
Jing, Q.-L., Liu, M.-J., Zhang, Z.-B., Fang, L.-Q., Yuan, J., Zhang, A.-R., et al. (2020). Household secondary attack rate of covid-19 and associated determinants in guangzhou, China: A retrospective cohort study. *The Lancet Infectious Diseases, 20*(10), 1141–1150.
Kada, D., Kouidere, A., Balatif, O., Rachik, M., & Labriji, E. H. (2020). Mathematical modeling of the spread of covid-19 among different age groups in Morocco: Optimal control approach for intervention strategies, chaos. *Solitons & Fractals, 141*, Article 110437.
Kissler, S. M., Kishore, N., Prabhu, M., Goffman, D., Beilin, Y., Landau, R., et al. (2020). Reductions in commuting mobility correlate with geographic differences in sars-cov-2 prevalence in new york city. *Nature Communications, 11*(1), 4674.
Martin, H., Wiedemann, N., Reck, D. J., & Raubal, M. (2023). Graph-based mobility profiling. *Computers, Environment and Urban Systems, 100*, Article 101910.
Mauro, G., Luca, M., Longa, A., Lepri, B., & Pappalardo, L. (2022). Generating mobility networks with generative adversarial networks. *EPJ data science, 11*(1), 58.
Monod, M., Blenkinsop, A., Xi, X., Hebert, D., Bershan, S., Tietze, S., et al. (2021). Age groups that sustain resurging covid-19 epidemics in the United States. *Science, 371*(6536), Article eabe8372.
Moreno, Y., Pastor-Satorras, R., & Vespignani, A. (2002). Epidemic outbreaks in complex heterogeneous networks. *European Physical Journal B: Condensed Matter and Complex Systems, 26*, 521–529.
Nicola, M., Alsafi, Z., Sohrabi, C., Kerwan, A., Al-Jabir, A., Iosifidis, C., et al. (2020). The socio-economic implications of the coronavirus pandemic (covid-19): A review. *International Journal of Surgery, 78*, 185–193.
Nouvellet, P., Bhatia, S., Cori, A., Ainslie, K. E., Baguelin, M., Bhatt, S., et al. (2021). Reduction in mobility and covid-19 transmission. *Nature Communications, 12*(1), 1090.
Ojugo, A. A., & Nwankwo, O. (2021). Modeling mobility pattern for the corona-virus epidemic spread propagation and death rate in Nigeria using the movement-interaction-return model. *International Journal, 9*(6).
Pardo-Araujo, M., García-García, D., Alonso, D., & Bartumeus, F. (2023). Epidemic thresholds and human mobility. *Scientific Reports, 13*(1), Article 11409.
Patel, M. D., Rosenstrom, E., Ivy, J. S., Mayorga, M. E., Keskinocak, P., Boyce, R. M., et al. (2021). Association of simulated covid-19 vaccination and non-pharmaceutical interventions with infections, hospitalizations, and mortality. *JAMA Network Open, 4*(6), Article e2110782–e2110782.
Pinheiro, C. A. R., Galati, M., Summerville, N., & Lambrecht, M. (2021). Using network analysis and machine learning to identify virus spread trends in covid-19. *Big Data Research, 25*, Article 100242.
Roy, S., Biswas, P., & Ghosh, P. (2021). Effectiveness of network interdiction strategies to limit contagion during a pandemic. *IEEE Access, 9*, 95862–95871.
Thompson, R. N., Stockwin, J. E., van Gaalen, R. D., Polonsky, J. A., Kamvar, Z. N., Demarsh, P. A., et al. (2019). Improved inference of time-varying reproduction numbers during infectious disease outbreaks. *Epidemics, 29*, Article 100356.
Vedam, N., & Ghose, D. (2022). The impact of mobility and interventions on the spread of diseases. *IEEE Transactions on Computational Social Systems, 10*, 5, 2291–1311.
Zhang, H., Yin, L., Mao, L., Mei, S., Chen, T., Liu, K., et al. (2022). Combinational recommendation of vaccinations, mask-wearing, and home-quarantine to control influenza in megacities: An agent-based modeling study with large-scale trajectory data. *Frontiers in Public Health, 10*.